

Raman spectral study of silicon nanowires

Bibo Li, Dapeng Yu, and Shu-Lin Zhang*

Department of Physics, Peking University, Beijing 100871, China

(Received 1 July 1998)

Raman spectra of silicon nanowires (Si NW's) have been analyzed, and the observed Raman peaks were assigned. The typical features of the first-order Raman peaks of the optical phonons were found matching those predicted by the quantum confinement effect. However, the sizes of Si NW's, derived from the microcrystal model (MCM) of Raman spectra do not fit the usual confined size, the diameter, of the nanowires from transmission electron microscope images. Abundant structure defects can be observed in Si NW's so that the Si NW's actually consist of many smaller Si grains. The size of such Si grains was found to give a better agreement with the size derived from the Raman spectra. This indicates that MCM can be used to interpret the Raman spectrum of Si NW's as long as one takes into account the influence of defect on the confined size. [S0163-1829(99)01303-X]

In pursuit of a variety of potential novel applications, many nanoscale materials have been fabricated.¹⁻⁵ Understanding the properties of these materials is both necessary and crucial for device applications and provides a formidable challenge. Raman spectroscopy plays an increasingly important role in the study of nanoscale materials. This is mainly due to the many advantages offered by the development of the micro-Raman technique. For example, only a microscopic amount of sample and low-power laser (about 20 mW) is needed and the measurement is very simple, fast, and inexpensive, with no damage to the sample.

The intrinsic Raman spectrum of one-dimensional nanoscale Si materials such as *p*-type porous silicon (PS) has been observed and interpreted based on the microcrystal model (MCM) successfully.^{6,7} Recently, another one-dimensional nanoscale Si material, silicon nanowires (Si NW's) has been synthesized by the laser ablation of metal-containing Si powder target.⁸⁻¹⁰ It is very interesting to find out the intrinsic Raman spectrum of this kind of one-dimensional nanoscale Si material and then to compare their Raman features with those of PS, another kind of one-dimensional nanoscale Si material. There is, to our knowledge however, no report on this project to date. In this paper, we present the results of our Raman investigation of these Si NW's.

The Si NW samples *A* and *B* in this study were synthesized by laser ablation^{8,9} under different growth conditions, so they have different diameter distributions. The transmission electron microscope (TEM) images of *A* and *B* are shown in Figs. 1(a) and 1(b), respectively. From the micrographs, it is estimated that 99% of the product in both samples are Si nanowires.⁹ Nanowires in sample *A* have an extremely uniform diameter of $13 \text{ nm} \pm 3 \text{ nm}$, and those in sample *B* have a diameter distribution from 15 to 60 nm. (The size-distribution effect on phonon Raman spectrum has been observed and will be published elsewhere. In this paper the discussion will be limited in the average size.) The thin outer layers of Si NW's were found overcoated with a thin layer of amorphous silicon oxide. The control sample of nano-SiO₂ wires in our experiments was obtained using the same approach as Si NW's. Crystalline silicon (*c*-Si) was

from commercial and used directly. Raman spectra of all samples were measured with a Renishaw system 1000 Raman microscope at room temperature. Excitation was done with the 632.8-nm line of a He-Ne laser. No polarizer was used and Raman signals were measured in a back-scattering geometry with a spectral resolution of 1.0 cm^{-1} .

The Raman spectra of *c*-Si, Si NW *A*, Si NW *B*, and nano-SiO₂ are shown in Figs. 2(a), 2(b), 2(c), and 2(d), respectively. A Raman peak at 520 cm^{-1} with the full width at half maximum (FWHM) of 2.8 cm^{-1} can be seen in the Raman spectrum of *c*-Si [Fig. 2(a)]. This is due to the scattering of the first-order optical phonon of *c*-Si. In addition, there are two broad peaks at ~ 300 and 970 cm^{-1} , respectively, which are from the scattering of two transverse acoustic (2TA) phonons and two transverse optical (2TO) phonons, respectively.¹¹ The Raman spectrum of nano-SiO₂ wires [Fig. 2(d)] contains an asymmetrical peak at $\sim 460 \text{ cm}^{-1}$ with a sharp peak at 490 cm^{-1} . In addition, there are two

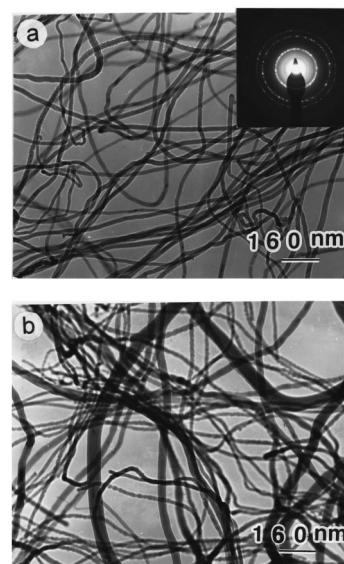


FIG. 1. (a) TEM micrograph of Si NW *A*. (b) TEM micrograph of Si NW *B*.

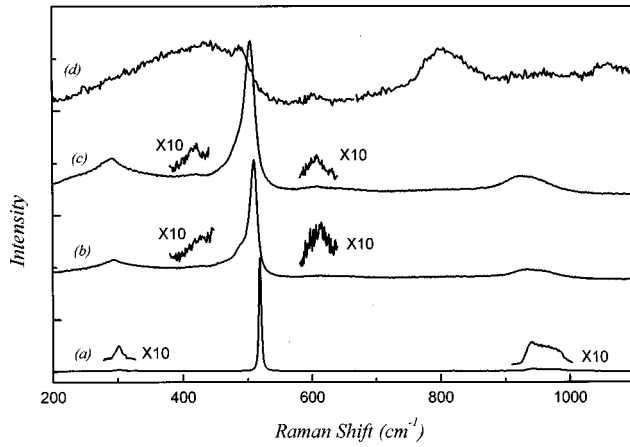


FIG. 2. Raman spectra of (a) *c*-Si, (b) Si NW B, (c) Si NW A, (d) nano-SiO₂ wires.

broad Raman features at ~ 800 and 1050 cm^{-1} . These features may be identified as the counterparts of TO-LO pairs in vitreous SiO₂.¹² The Raman spectra of samples A and B in Figs. 2(b) and 2(c) show prominent Raman features at ~ 504 and 511 cm^{-1} , respectively, with a shoulder at 486 and 495 cm^{-1} , respectively. In addition, there are two broad peaks at ~ 950 and 290 cm^{-1} and two weak features at ~ 630 and 450 cm^{-1} . None of these features in Figs. 2(b) and 2(c) can be attributed to those in Fig. 2(d) of nano-SiO₂. This indicates that the spectra in Figs. 2(b) and 2(c) do not have contribution from nano-SiO₂ even though SiO₂ surrounds the Si NW's. In contrast, comparing the Raman spectra of Si NW's with that of *c*-Si, shows that, except for two weak features at ~ 630 and 450 cm^{-1} , these spectra are quite similar with only minor differences. In comparison with the first-order optical phonon peak of *c*-Si, the corresponding Raman peak of Si NW's has its frequency down-shifted, its linewidth broadened and its line shape becomes asymmetric. Moreover, we also found for the two obvious peaks of Si NW's that the frequencies shift a lot and the relative intensities increase much related to those of 2TO and 2LO modes of *c*-Si. These features and the appearance of two weak peaks at ~ 630 and 450 cm^{-1} in the spectra of Si NW's are expected the typical characteristics of nano-crystalline¹³ and porous silicon,^{6,7,11} which can be ascribed to the quantum confinement effect of Si. Therefore, we may identify the spectra in Figs. 2(b) and 2(c) as the intrinsic Raman spectra of Si NW's and may consider them due to the quantum confinement effect.

We will concentrate on the changes in the first-order optical mode. Qualitatively, when the crystalline size decreases, momentum conservation will be relaxed and Raman active modes will not be limited to be at the center of the Brillouin zone.¹³ The smaller the crystalline grain is, the bigger the frequency shifts and the more asymmetric and the broader the peak becomes. This feature has been confirmed by experiments on microcrystalline silicon¹³ and porous silicon.⁷ Table I lists the spectral parameters of the first-order optical phonon spectra of Si NW's and *c*-Si as well as sizes of Si NW's. The spectral parameters are the Raman frequency, the frequency shift compared to the Raman frequency of *c*-Si, the FWHM, the coefficient of broadening (C_b) defined by $\text{FWHM}_{\text{Si NW's}}/\text{FWHM}_{c\text{-Si}}$, and the asymmetric coefficient (C_a) defined as LWHM/RWHM , where LWHM and RWHM are the left width at half maximum and the right width at half maximum from the central peak position, respectively. From Table I, we found that the frequency shift, the coefficient of broadening C_b , and the asymmetric coefficient C_a of sample A are all larger than those of sample B. This is expected qualitatively from the values in the order of size measured by TEM listed in Table I, giving further support to that the Raman spectra shown in Figs. 2(b) and 2(c) result from the quantum confinement effect of the Si NW samples A and B.

The MCM based on the quantum confinement effect has been successfully applied to many nanoscale materials.^{7,14,15} According to MCM, the theoretical first-order Raman spectrum can be obtained from the following equation:¹⁶

$$I(\omega) = \int \frac{d^3q C(0,q)^2}{[\omega - \omega(q)]^2 + \left(\frac{\Gamma_0}{2}\right)^2}, \quad (1)$$

where $\omega(q)$ is the phonon dispersion curve (q , the phonon wave vector); Γ_0 is the natural linewidth (inversely proportional to the intrinsic phonon lifetime); $C(0,q)$ is the coefficient describing the phonon confinement at $q_0=0$, which is appropriate for first-order Raman scattering. The integration must be performed over the entire Brillouin zone. After fitting with various forms of $C(0,q)$, we found that the best confinement function is a Gaussian one:

$$C(0,q) = \exp\left(-\frac{q^2 L^2}{4\pi^2}\right), \quad (2)$$

TABLE I. The Raman frequency, the frequency shift from the Raman frequency of *c*-Si, the FWHM, the coefficient of broadening (C_b) defined by $\text{FWHM}_{\text{Si NW's}}/\text{FWHM}_{c\text{-Si}}$, the asymmetric coefficient (C_a) defined as LWHM/RWHM [the left width at half maximum (LWHM) and the right width at half maximum (RWHM) from the central peak position] as well as the sizes of the diameter measured by TEM, the sizes calculated by the Raman spectra, and the sizes of the grain measured by TEM.

Samples	Raman frequency (cm^{-1})	Frequency shift (cm^{-1})	FWHM (cm^{-1})	C_b	C_a	TEM size of diameter (nm)	Raman size (nm)	TEM size of grain (nm)
Si NW A	504	18	23.1	8.3	1.41	13	9.5	10
Si NW B	511	9	15.6	5.6	1.11	20	13.0	15
<i>c</i> -Si	520	0	2.8	1	1			

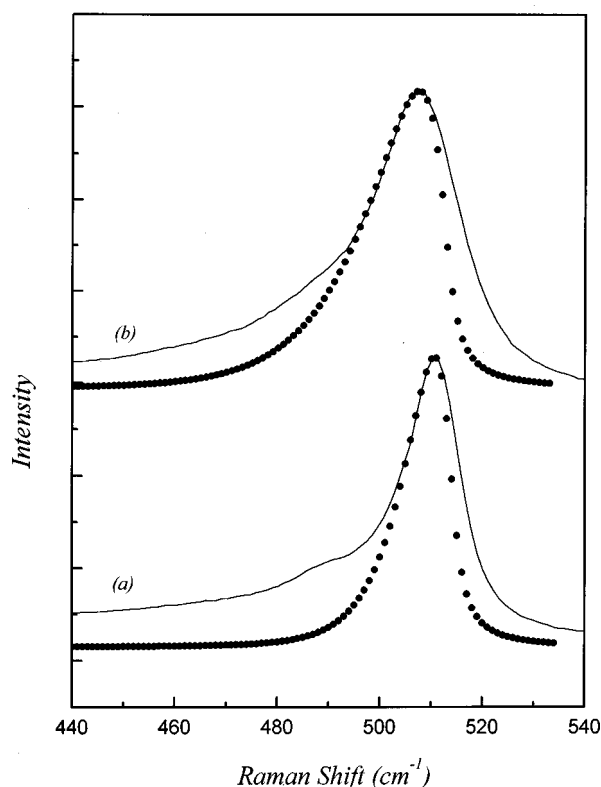


FIG. 3. Comparison of measured and calculated first-order Raman spectra of (a) Si NW B, (b) Si NW A.

where L is the size of crystals. The result of fitting the first-order optical phonon mode using MCM is shown in Fig. 3. The fitted L values by Raman data are listed in Table I. There is good general agreement in spectral features between experimental and calculated Raman spectra, indicating that the identification of Raman peak at ~ 504 and 511 cm^{-1} in Figs. 2(b) and 2(c) is correct.

On closer examination, however, several discrepancies are found between theoretical and experimental spectra in Fig. 3. First, the calculated spectra do not cover the features of both low- and high-frequency sides with the shoulders at ~ 486 cm^{-1} for Si NW B and 495 cm^{-1} for Si NW A, suggesting that there are other components not due to Si NW's. They may be attributed to the amorphous silicon that covers Si NW's, which has a Raman structure between 400 and 550 cm^{-1} with a peak at ~ 480 cm^{-1} .¹³ Second, the sizes of Si NW's derived from the Raman spectra are up to 3.5 nm smaller than those obtained by TEM (see Table I). The second discrepancy questions the validity of using the MCM to interpret our experimental results. In general, lattice distortion and structure defects are the common features of most nanostructured materials. In our Si NW samples, abundant structure defects can be also found in the high resolution TEM images, such as stacking defaults and twins.¹⁰ The

presence of defects can have profound influence on the Raman spectra. First, this may introduce new defect Raman mode. However, we cannot assign any new Raman structure to the defects in Figs. 2(b) and 2(c), which indicates that the defects have no significant direct effect on the Raman spectra of our Si NW's. Second, the existence of defects results in breaking up the nanowires with a certain diameter into smaller grains with typical dimension of only a few nms. One usually considers the diameter of the nanowires as the confined size. This is the case for porous silicon (PS) and MCM is a good model to interpret the first-order Raman spectrum using the diameter of PS nanowires.⁷ This is due to the fact that PS is prepared on a wafer of c -Si and the inner part of remnant Si units of PS still maintain the c -Si lattice. However, for Si NW's, the wire in most cases is not the perfect lattice on the whole. Therefore, the confined size should be that of the grains that make up the Si NW's rather than the diameter of Si NW's. With this in mind, we measured the size of all grains in the TEM images and averaged them to obtain the mean grain size of the two samples to be 10 and 15 nm, respectively (see Table I). These values match very well with the sizes calculated from the Raman spectra, confirming that the present MCM is still valid in interpreting the Raman spectra of Si NW's. Note that the phonon density of states (DOS) is not taken into account in the MCM represented by formula (1). This suggests that the observed first-order Raman spectra can be attributed to the phonon peaks rather than the phonon DOS. Therefore, this indicates that the long-range order may not be lost in this one-dimensional system.¹⁷

In conclusion, we have observed and identified the Raman peaks of Si NW's. The features of the observed Raman spectra of two samples of Si NW's with different sizes qualitatively match those predicted by the quantum confinement model for Si microcrystals. A detailed calculation using the microcrystal model to interpret the observed first-order Raman spectra shows a significant disagreement of the confined size with the diameter observed by TEM. This discrepancy is resolved by recognizing that the Si NW's are actually consisted of a collection of smaller crystalline grains due to the presence of abundant structure defects. Thus, the effective confined size is not the diameter of the wires. We measured the average sizes of Si grains in Si NW's from their TEM images and found that they fit the corresponding sizes extracted from the Raman spectra using MCM. The result indicates that MCM is still valid for NW's but one must use the appropriate grain size as the confined size.

We acknowledge financial support from NSFC under Grants Nos. 69476037 and 19774009 and the State Commission of Science and Technology. We thank Dr. K.T. Yue for helpful discussion and Lixia Zhou and Lu Sun for technical assistance.

*Author to whom correspondence should be addressed. Electronic address: slzhang@pku.edu.cn

¹S. Iijima, *Nature (London)* **354**, 56 (1991).

²N. Hatta and K. Murata, *Chem. Phys. Lett.* **217**, 398 (1994).

³Hongjie Dai, Eric W. Wong, Yuan Z. Lu, Shoushan Fan, and Charles M. Lieber, *Nature (London)* **375**, 769 (1995).

⁴R. W. Hausslein (unpublished).

⁵W.Z. Li, S. S. Xie, and L.X. Qian, *Science* **274**, 1701 (1996).

⁶Z. Sui, P.P. Leong, I.P. Herman, G.S. Higasi, and X. Temkin, *Appl. Phys. Lett.* **60**, 2085 (1992).

⁷Shu-Lin Zhang, Yongtian Hou, Kuok-San Ho, Bidong Qian, and Shengmin Cai, *J. Appl. Phys.* **72**, 44 613 (1992).

- ⁸D.P. Yu, C.S. Lee, I. Bello, G.W. Zhou, and Z.G. Bai, Solid State Commun. **105**, 403 (1998).
- ⁹D.P. Yu, X.S. Sun, C.S. Lee, I. Bello, S.T. Lee, H.D. Gu, K.M. Leung, G.W. Zhou, Z.F. Dong, and Z. Zhang, Appl. Phys. Lett. **72**, 1966 (1998).
- ¹⁰G.W. Zhou, Z. Zhang, Z.G. Bai, S.Q. Feng, and D.P. Yu, Appl. Phys. Lett. **73**, 677 (1998).
- ¹¹S.L. Zhang, X. Wang, K. Ho, Jinjian Li, Peng Diao, and Sheng-min Cai, J. Appl. Phys. **76**, 3061 (1994).
- ¹²F.L. Galeener and G. Lucovsky, Phys. Rev. Lett. **37**, 1474 (1976).
- ¹³Z. Iqbal and S. Veprek, J. Phys. C **15**, 377 (1982).
- ¹⁴R.J. Nemanich, S.A. Solin, and R.M. Martin, Phys. Rev. B **23**, 625 (1981).
- ¹⁵H. Richter, Z.P. Wang, and L. Ley, Solid State Commun. **39**, 625 (1981).
- ¹⁶I.H. Campbell and P.M. Fauchet, Solid State Commun. **39**, 625 (1981).
- ¹⁷R. Shuker and R. W. Gammom, Phys. Rev. Lett. **25**, 222 (1970).